The scalability of gadolinium-doped water-Cherenkov detectors for nonproliferation

Viacheslav A. Li[1]

Lawrence Livermore National Laboratory, Livermore, CA 94550

Abstract

Among other applications, antineutrino detection offers a remote but still cooperative capability to discover or exclude operating nuclear reactors in relatively large geographic regions. The non-intrusiveness of this approach may be attractive to the country being monitored, while its persistence, wide areal coverage, and well-defined criteria for discovery or exclusion, and the opportunities it provides for scientific engagement and open dissemination of data, may be attractive to inspecting parties and the international community.

Here we report the main findings of a recent study of the reactor-discovery potential for a specific technology: large-volume Gd-doped-water Cherenkov detectors. Realistic background models for the worldwide reactor flux, geoneutrinos, cosmogenic fast neutrons, and detector-associated backgrounds are included. We calculate the detector run time required to detect a small 50-MWt reactor at a variety of stand-off distances as a function of detector size. We also discuss possible improvements that could lead to increased standoff, reduced dwell-time or other operational advantages.

In proceedings of the joint Institute of Nuclear Materials Management (INMM) and the European Safeguards Research and Development Association (ESARDA) Annual Meeting, May 22–26, 2023, Vienna, Austria.

[1]E-mail: li68@llnl.gov

1 Antineutrinos and their role in reactor monitoring

Fission nuclear weapons use uranium and plutonium. Plutonium is advantageous as it has a lower critical mass than uranium. Plutonium is made in a nuclear reactor by irradiating uranium [1]. New reactor designs such as small modular reactors might require new methods of safeguarding them [2, 3]. In addition, geopolitical tensions could create scenarios where access to the facilities is limited, making it difficult or impossible to assess the amount of plutonium that was made [4].

Nuclear reactors emit an enormous number of antineutrinos. In a single fission reaction, about 200–210 million of electron-volts are released and about 6 antineutrinos are emitted as a result of fission-product beta decays. In other words, roughly 2×10^{17} antineutrinos are emitted per second per 1 MW of reactor's thermal power. Neutrinos and their antiparticles, antineutrinos, are weakly interacting particles with an extremely low interaction cross section [5, 6]. For the inverse-beta-decay (IBD) reaction:

$$\bar{\nu}_e + p \rightarrow e^+ + n, \tag{1}$$

the cross section is of the order of 10^{-44}cm^2 for an MeV-scale antineutrino; which in turn results in a mean free path on the order of a thousand of light years in water.

The IBD reaction Eq. 1 has a 1.8-MeV threshold. About 1/4 of emitted reactor antineutrinos are above the threshold. Thus, in a thousand tonnes of water, the interaction rate is roughly 1 event per day for a flux of neutrinos for a 50-MWt reactor at 2 km.

Neutrinos were first detected at a nuclear reactor using the IBD reaction and a delayed-coincidence technique in 1956 by Reines and Cowan collaboration, 26 years after being first proposed by Pauli. In 1960, Markov proposed to use large bodies of water to detect high-energy neutrinos by using Cherenkov radiation from the neutrino-induced charged lepton, such as an electron or muon [7]. This idea was central to the DUMAND and Baikal neutrino telescopes, and subsequently led to IceCube. To lower the detection threshold, a higher photo coverage and better background suppression are needed, not achievable in open water. The pioneering underground water-Cherenkov detectors IMB and Kamiokande were sensitive to the burst of neutrinos emitted from SN1987A using elastic neutrino-electron scattering reaction in the tens of MeV range. However, without a special dopant, the backgrounds would need to be substantially lower to be sensitive to the IBD reaction (such that originate from reactor antineutrino interactions). The detection of reactor antineutrinos in an undoped water was not realized until last year, in the water-phase of the SNO+ detector, a remarkable achievement — sensitivity to CANDU reactors few hundred kilometers away from the detector [8].

In 1977, it was noted that reactor antineutrino signal might have a utility for monitoring purposes [9]. A series of experiments were successful in observing fuel burn-up using reactor antineutrino radiation.

Going into far field (10s of kilometers) required some clever engineering, underground facilities, and relatively large detector volumes. KamLAND, an undoped 1-kton liquid-scintillator detector, was the first to be sensitive to reactor antineutrinos in the far field, and was able to confirm the phenomenon known as neutrino oscillations [10]. It was sensitive to pick up signals from reactors few hundred kilometers away.

In early 2000s, it was proposed to dope water with gadolinium in large detectors in order to improve sensitivity to the IBD reaction [11, 12]. In late 2010s, Super-Kamiokande began introducing gadolinium to the pure DI water. The first phase of doping was recently completed [13].

A series of workshops dedicated to discussion of applications behind neutrino physics have been ongoing for nearly two decades [14]. Another detector sensitive to far field is JUNO [15], a liquid scintillator detector. Once constructed it will be sensitive to reactors beyond 50 km.

2 Study to assess scalability of Gd-water detectors

In our recent study [16], we determine the scalability of detectors filled with Gd-water and the range over which a relatively small reactor can be detected in the presence of realistic backgrounds (world-reactors and detector-related backgrounds). Since the number of events generally follow the inverse square of distance, it is natural to expect that the range would scale approximately with the square root of detector mass and linearly with the reactor power:

$$\text{range} \propto \sqrt{m_{\text{det}}} \tag{2}$$

$$\text{range} \propto \text{power} \tag{3}$$

First, we select the detection medium. Water is an abundant resource, and recent advances in doping large water detectors with gadolinium are highly encouraging.

Second, we select geographic location to account for realistic world-reactor backgrounds, as well as geo-neutrinos; although the latter doesn't affect much as we show later.

Third, we then model the detector performance using a specially designed toolkit called RAT-PAC, which is based on GEANT4. We include the following realistic detector performance parameters — water attenuation, PMT quantum efficiency and noise rates, detector component radiopurity levels, etc.

Finally, we apply the detectability metric to estimate dwell time and range to detect a test reactor.

Since our presentation at INMM 2019 [17], a series of related studies on the subject of reactor antineutrinos and non-proliferation in the context of far field have been published. Here, we briefly reference them. Various subgroups of AIT/WATCHMAN collaboration have assessed various scenarios and detector fills for the sensitivity of a detector placed in the Boulby Mine in the United Kingdom. That included a detector with two different fills: a Gd-water and water-based liquid scintillator. A variety of new techniques were explored, such as ranging, directionality, and new reconstruction algorithms[18–23].

3 Gadolinium-doped water and inverse beta decay

The positron energy from the IBD reaction is correlated with the antineutrino energy. The positron travels a distance on the order of a centimeter before annihilating into two gamma rays: The positron produces Cherenkov light if its energy is above $\sim$ 260-keV. The Cherenkov photons are emitted at an angle $\cos\theta = c/(nv)$ relative to the direction of motion of a charged particle moving at speed v in medium with index of refraction n; in water, the angle is $\lesssim 41^\circ$ [24].

After the annihilation with an electron, the 511-keV gamma-rays Compton scatter off electrons. The latter generally don't have sufficient energy to be detectable in a water Cherenkov detector.

Neutrons from the IBD reaction have a kinetic energy in the tens of keV range. Carrying no electrical charge, they do not produce any Cherenkov radiation. After a number of elastic scatters, they loose energy and eventually thermalize. As they loose energy, the neutron capture cross section increases, capturing on hydrogen or on a dopant element. Two isotopes of gadolinium, 155 and 157, have enormously high thermal-neutron-capture cross sections, the highest of any known stable nuclei. After capturing on gadolinium, a few gamma rays are emitted with a total of about 8 MeV of energy. The Compton-scattered electrons resulting from these gamma-rays have sufficient energy to produce Cherenkov radiation and be detectable in water.

4 Geographic location and world reactors

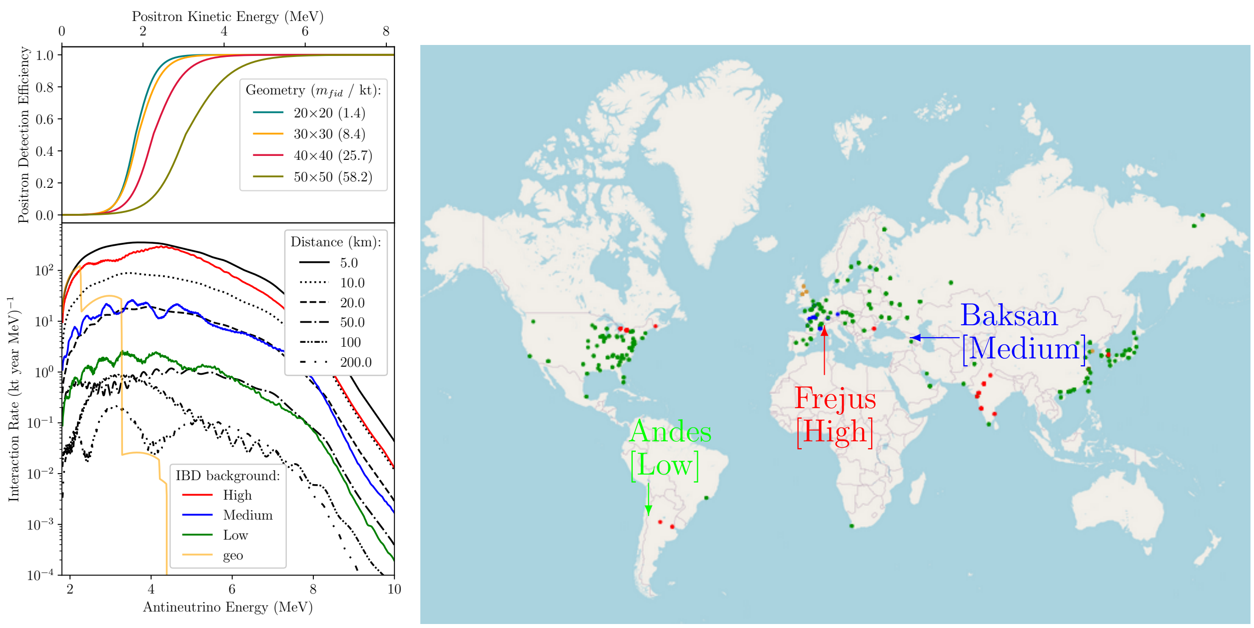

Figure 1: *Left:* IBD spectra of the three representative locations shown in the right panel. The 50-MWt reactor spectra for different stand-offs are also shown. *Right:* Map of world power reactors, taken from geoneutrinos.org. Legend: red — pressurized-heavy-water reactor (PHWR, mostly in Canada and India); green — pressurized-water reactor (PWR); blue — PWR with mixed-oxide fuel (mostly in France); orange — gas-cooled reactors (mostly in the UK). The three detector locations used in this study are shown, indicating three levels of world-reactor backgrounds: Andes (low), Baksan (medium), Frejus (high). Those locations are used as representative of world-reactor background levels, *not* overburden.

The three locations used in this study (shown in Fig. 1) are to represent typical world-reactor backgrounds [25], and are not indicative of the overburden used in this study. In the far field (distances > 10 km), neutrino oscillations become a significant effect and need to be taken into account. The result is a distortion of the spectrum and an overall suppression of event rate — roughly 20% of the original 5-MeV neutrinos "survive" at 80 km (Fig. 2).

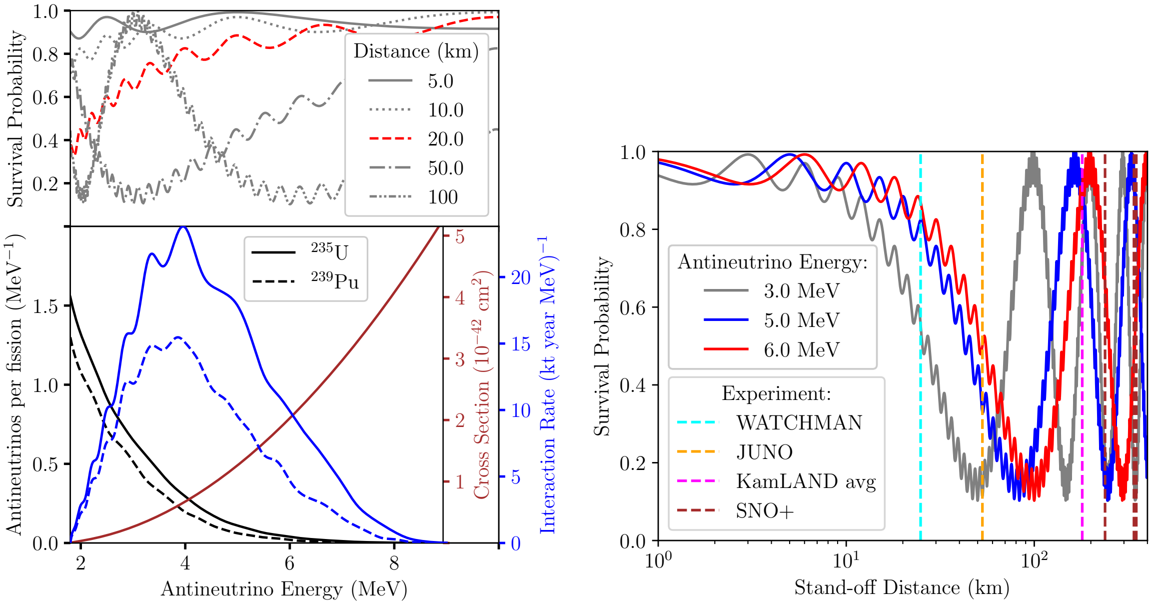

Figure 2: *Left:* Reactor antineutrino survival probability as a function of energy for selected baselines (top panel); emitted and detector spectra. *Right:* Neutrino oscillations in the far field. Several ongoing and proposed detectors are shown.

5 Detector geometry and associated backgrounds

A set of Gd-water detector of various sizes were simulated. The detectors simulated were right cylinders with 40% photocoverage. The detector-associated backgrounds were modeled based on realistic radiopurity levels found in purified water and PMT glass. A series of cuts were applied to select candidate IBD events. Although geological antineutrinos are included, they do not pose a substantial background since they are mostly below the detector threshold. To estimate fast-neutron rates, which depend on depth, the detector overburden is fixed at 2.8 km.w.e. (roughly 1 km underground). This is the depth of the Boulby mine in Northern England, a site once contemplated for the deployment of a water-based detector for reactor monitoring. The Mei-Hime model can be used to predict neutron backgrounds for different overburdens. [26]. A series of different sized detectors were simulated, and their sensitivity to a 50-MWt reactor assessed at various stand-off distances.

6 Dwell time and range

As a sensitivity metric, we apply Minimum Detectable Amount metric described in Knoll's textbook [27]:

$$N_D = 4.653\sqrt{N_B} + 2.706 \tag{4}$$

$$s\,t = 4.653\sqrt{b\,t} + 2.706 \tag{5}$$

which can roughly be interpreted as follows: if we have 100 background events, we will need at least 50 signal events for a positive detection. The metric assumes the use of Gaussian statistics, and therefore is applicable when any of the N_D or N_B is greater than ~ 30. To account for different reactor power levels, one can apply a scaling factor $X/50$ in front of the N_D term, where X is a reactor power in MWt.

We solve for time t based on the metric in Eq. 5, and then calculate range by fixing a dwell time to 1 year. The final plot is shown in Fig. 3.

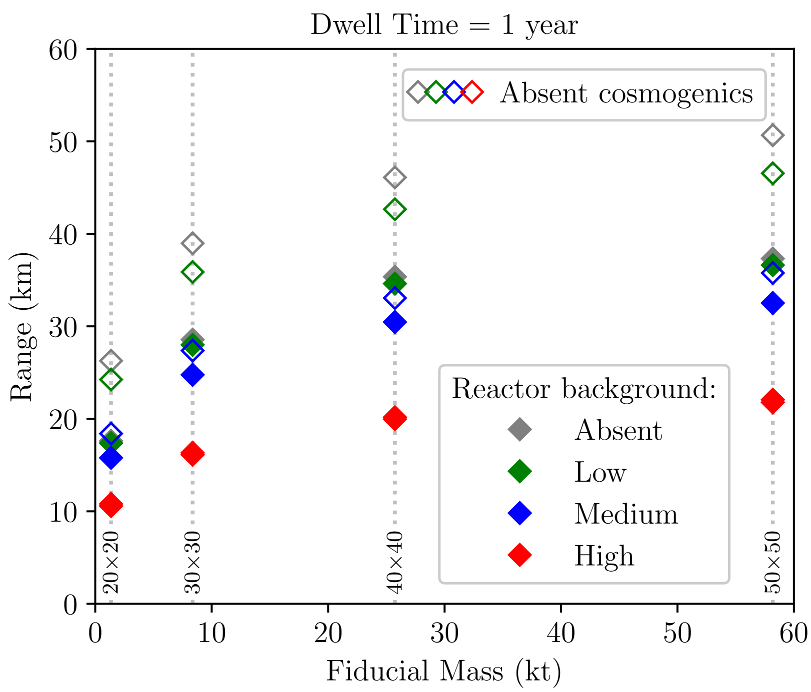

Figure 3: Maximum range as a function of detector fiducial mass for a 1-year dwell time at the three representative world-reactor backgrounds (See text). The empty rhombi indicate scenarios with zero cosmogenic fast-neutron backgrounds - the limit one can achieve with depth. The geographic locations for the three representative world-reactor backgrounds are shown in Fig. 1.

One can also use this study to find dwell times for other reactor powers. Solving the Eq. 5 for t, one obtains the following approximation:

$$t = \frac{9\left(31\sqrt{961b^2 + 480bs} + 961b + 240s\right)}{800s^2} \tag{6}$$

For example, if the background rate b is 4000 events per year (roughly corresponds to the 50×50 detector placed in the high world-reactor background), then the dwell time to detect a 50-MWt reactor at a 20-km standoff (signal rate s is about 400 events per year), is about half a year. However, if the power of the reactor is 150-MWt (multiply s by a factor of 3) at the same standoff, then the dwell time is roughly 1 month.

7 Conclusion and outlook

Although large scale antineutrino detectors require a substantial capital investment and cooperation to be built, they nevertheless could serve as a viable option for a cooperative reactor monitoring of a certain region. First steps to simulate realistic detector performance have been taken. Next steps might involve investigating new techniques and out-of-the-box thinking on how to extend the range.

8 Acknowledgement

This work was performed under the auspices of the U.S. Department of Energy by Lawrence Livermore National Laboratory under Contract DE-AC52-07NA27344. Release number LLNL-PROC-848616.

References

[1] B. T. Goodwin. Nuclear Weapons Technology 101 for Policy Wonks. *LLNL CGSR*, 2021.

[2] Advances in Small Modular Reactor Technology Developments. *A Supplement to IAEA Advanced Reactors Information System (ARIS) aris.iaea.org*, 2022.

[3] S. E. Bays, G. A. Reyes, M. J. Schanfein, R. H. Stewart, and N. P. Martin. Significant Quantity Production Rates in Small Modular Reactors. *Proceedings of the INMM and ESARDA Joint Virtual Annual Meeting*, 2021.

[4] S. S. Hecker. *Hinge Points: An Inside Look at North Korea's Nuclear Program.* Stanford University Press, 2023.

[5] F. Reines. The Neutrino: From Poltergeist to Particle. *Nobel Lecture*, 1995.

[6] J. A. Formaggio and G. P. Zeller. From eV to EeV: Neutrino Cross Sections Across Energy Scales. *Rev. Mod. Phys.*, 84:1307–1341, 2012.

[7] M. A. Markov. On High Energy Neutrino Physics. In *10th International Conference on High Energy Physics*, pages 578–581, 1960.

[8] A. Allega et al. Evidence of Antineutrinos from Distant Reactors Using Pure Water at SNO+. *Phys. Rev. Lett.*, 130:091801, 2023.

[9] L. A. Mikaelyan. Neutrino Laboratory in the Atomic Plant (Fundamental and Applied Researches). In *Neutrino 77 Proceedings*, volume 2, page 383, 1978.

[10] K. Eguchi et al. First results from KamLAND: Evidence for reactor anti-neutrino disappearance. *Phys. Rev. Lett.*, 90:021802, 2003.

[11] A. Bernstein, Y. Wang, G. Gratta, and T. West. Nuclear reactor safeguards and monitoring with anti-neutrino detectors. *J. Appl. Phys.*, 91:4672, 2002.

[12] J. F. Beacom and M. R. Vagins. Anti-neutrino spectroscopy with large water Cherenkov detectors. *Phys. Rev. Lett.*, 93:171101, 2004.

[13] K. Abe et al. First gadolinium loading to Super-Kamiokande. *Nucl. Instrum. Meth. A*, 1027:166248, 2022.

[14] Applied Antineutrino Physics Workshops, www.phys.hawaii.edu/aap/ (2004–present). *University of Hawai'i, online repository.*

[15] A. Abusleme et al. JUNO physics and detector. *Prog. Part. Nucl. Phys.*, 123:103927, 2022.

[16] V. A. Li, S. A. Dazeley, M. Bergevin, and A. Bernstein. Scalability of Gadolinium-Doped-Water Cherenkov Detectors for Nuclear Nonproliferation. *Phys. Rev. Appl.*, 18:034059, 2022.

[17] V. A. Li. Far-Field Monitoring of Reactor Antineutrinos for Nonproliferation. *Proceedings of the INMM 60th Annual Meeting, arXiv:1907.08891*, 2019.

[18] D. L. Danielson et al. Directionally Accelerated Detection of an Unknown Second Reactor with Antineutrinos for Mid-Field Nonproliferation Monitoring. *arXiv:1909.05374*, 2019.

[19] E. Kneale, S. T. Wilson, T. Appleyard, J. Armitage, N. Holland, and M. Malek. Sensitivity of an antineutrino monitor for remote nuclear reactor discovery. *arXiv:2210.11224*, 2022.

[20] A. Mullen, O. Akindele, M. Bergevin, A. Bernstein, and S. Dazeley. Improvement in light collection of a photomultiplier tube using a wavelength-shifting plate. *Nucl. Instrum. Meth. A*, 1040:167207, 2022.

[21] E. Kneale, M. Smy, and M. Malek. Coincidence-based reconstruction for reactor antineutrino detection in gadolinium-doped Cherenkov detectors. *arXiv:2210.10576*, 2022.

[22] O. A. Akindele, A. Bernstein, M. Bergevin, S. A. Dazeley, F. Sutanto, A. Mullen, and J. Hecla. Exclusion and Verification of Remote Nuclear Reactors with a 1-kiloton Gd-Doped Water Detector. *Phys. Rev. Appl.*, 19:034060, 2023.

[23] S. T. Wilson, C. Cotsford, J. Armitage, T. Appleyard, N. Holland, M. Malek, and J. G. Learned. Remote Reactor Ranging via Antineutrino Oscillations. *arXiv:2303.16661*, 2023.

[24] L. D. Landau, E. M. Lifshitz, and L. P. Pitaevskii. *Electrodynamics of Continuous Media (2nd ed.)*. Pergamon Press, 1984.

[25] A. Barna and S. Dye. Global Antineutrino Modeling: A Web Application. *arXiv:1510.05633*, 2015.

[26] D. Mei and A. Hime. Muon-induced background study for underground laboratories. *Phys. Rev. D*, 73:053004, 2006.

[27] G. Knoll. *Radiation Detection and Measurement (4th ed.)*. Wiley, 2010.